

Strong-coupling perturbation theory for the two-dimensional Bose-Hubbard model in a magnetic field

M. Niemeyer[†], J. K. Freericks^{*}, and H. Monien[†]

[†]*Physikalisches Institut der Universität Bonn, Nußallee 12, D-53115 Bonn, Germany*

^{*}*Department of Physics, Georgetown University, Washington, D.C. 20057*

(October 9, 2018)

The Bose-Hubbard model in an external magnetic field is investigated with strong-coupling perturbation theory. The lowest-order secular equation leads to the problem of a charged particle moving on a lattice in the presence of a magnetic field, which was first treated by Hofstadter. We present phase diagrams for the two-dimensional square and triangular lattices, showing a change in shape of the phase lobes away from the well-known power-law behavior in zero magnetic field. Some qualitative agreement with experimental work on Josephson-junction arrays is found for the insulating phase behavior at small fields.

PACS numbers: 05.30.Jp, 05.70.Fh, 67.40.Db

I. INTRODUCTION

The simplest model of strongly interacting bosons is the Bose-Hubbard model (BHM), which has been used to describe superfluid helium¹, Cooper pairs in thin granular superconducting films² and Josephson junction arrays³. Much theoretical work has concentrated on the phase diagram of the BHM in zero magnetic field⁴ because of the technical problems associated with introducing an external magnetic field (such as the sign problem in quantum Monte Carlo simulations). Experimentalists on the other hand have concentrated on studying systems in an external magnetic field because the phase transition can be tuned by adjusting the magnetic field rather than changing the samples measured^{5,6}. We study the BHM on two-dimensional lattices in a perpendicular magnetic field by extending the strong-coupling perturbation theory for the field-free case⁷. This theoretical technique can incorporate magnetic-field dependence in a straightforward manner and is useful in studying field-tuned transitions. We concentrate on pure systems in this contribution and do not include any effects due to disorder. We present zero-temperature phase diagrams, study excitation-gap energies, calculate the dynamical critical exponent $z\nu$ for small fields, and compare our theoretical results with experimental ones.

The BHM contains the key physics of a many-particle bosonic system with competing potential and kinetic energy effects. The typical zero-temperature phase diagram for the non-magnetic case shows incompressible Mott-insulating (MI) phases surrounded by compressible superfluid phases (SF)⁴. The insulator to superfluid transitions at the tip of the lobes (where the density remains constant) are driven by quantum phase fluctuations, while those at the sides of the lobes (where the density varies) are driven by density fluctuations, i.e. particle or hole excitations. Introducing a magnetic field is expected to increase the region of the MI phase because the localizing effect on the itinerant bosons reduces the stability of the SF phase.

We consider bosons with total spin 0. The only effect of a perpendicular magnetic field \vec{H} is then on the orbital motion of the bosons, which effects changes in the phase of the hopping-matrix $\hat{T} = (t_{jk})$ between lattice sites j and k . By choosing a Landau-gauge for the vector-potential $\vec{A}(\vec{r}) = H(0, x, 0)$, the Bose-Hubbard Hamiltonian in an external magnetic field becomes

$$H_{BHM} = - \sum_{\langle jk \rangle} (t_{jk} b_j^\dagger b_k + h.c.) + \frac{U}{2} \sum_j \hat{n}_j (\hat{n}_j - 1) - \mu \sum_j \hat{n}_j, \quad (1)$$

where the hopping matrix is nonzero only between nearest neighbors and is given by

$$t_{jk} = t e^{-i2\pi \vec{A}_{jk}}, \quad \vec{A}_{jk} = \frac{1}{\phi_0} \int_j^k \vec{A}(\vec{r}) \cdot d\vec{r}. \quad (2)$$

This hopping matrix is Hermitian because t is real and $\vec{A}_{jk} = -\vec{A}_{kj}$. Here the boson creation operator for lattice site j is b_j^\dagger , $\hat{n}_j = b_j^\dagger b_j$ is the corresponding number operator, U is the on-site repulsion of the bosons, and μ is the chemical potential. We choose U to be our energy scale and measure all energies in units of U . The magnetic flux quantum is

given by $\phi_0 = \frac{hc}{e}$, and the magnetic flux per plaquette $2\pi\phi = \oint \vec{A}(\vec{r}) \cdot d\vec{r} \sim a^2 H$ is a measure of the strength of the magnetic field \vec{H} (where a is the lattice spacing).

The form of the zero-temperature phase diagram can be understood by starting from the atomic limit⁷, where the hopping t is zero and every site is occupied by a fixed number of bosons n_0 . The energy to add one boson onto a site with n_0 bosons is $E(n_0 + 1) - E(n_0) = n_0 U - \mu$, so that there is a finite energy gap when $(n_0 - 1)U < \mu < n_0 U$ and the system is an incompressible Mott insulator. When $\mu = n_0 U$, then all states with a density between n_0 and $n_0 + 1$ bosons per site are degenerate in energy, and the system becomes a compressible fluid. As the strength of the hopping matrix elements increases, the range of the chemical potential about which the system is incompressible decreases. The Mott insulator phase disappears at a critical value of the hopping matrix elements (which depends on the strength of the magnetic field and the density of the insulating phase) and the system becomes a superfluid (see Fig.2). We provide a systematic study of the BHM in a magnetic field by examining the system in a perturbative expansion about the atomic limit with the boson kinetic energy acting as the perturbation.

The paper is organized as follows: Section II describes the formalism used in the strong-coupling perturbation theory in the presence of a magnetic field. Section III presents the results for the phase diagrams and the excitation energies in a magnetic field, and Section IV contains the conclusions.

II. FORMALISM

Our procedure is to calculate the ground-state energy of the MI phase with n_0 bosons per site $E_g(n_0, t)$, and of the excited states in the charge sector with one extra boson $E_p(n_0, t)$ and one extra hole $E_h(n_0, t)$, in a Rayleigh-Schrödinger perturbative expansion in the hopping matrix element t (the kinetic energy is chosen as the perturbative part of the Hamiltonian). When the energy of the MI and the state with one extra boson are equal, the system undergoes a phase transition from the incompressible MI phase to the compressible SF phase with density larger than n_0 . The similar occurs when the state with one extra hole is degenerate with the MI phase (except now the density of the SF phase is less than n_0). The detailed formalism of the strong-coupling expansion for the ground-state energies has already been presented⁷. The only modifications of the previous calculations needed here are to take into account the fact that the hopping matrix now has a complex phase and the changes required for the nonbipartite hopping matrix of the triangular lattice. The important parameter that enters the results is the minimal eigenvalue ϵt of the kinetic energy matrix $-t_{jk}$ which includes a factor ϵ that depends on the magnetic field. This parameter determines how the degeneracy is lifted in the first-order secular equation for the energy of the excited states in the charge sector. Formally this solution of the minimal eigenvalue is identical to finding the band minimum in the Hofstadter problem⁸.

The Mott phase diagram is determined by the two Mott phase boundaries—one for the particle excitations [where $E_p(n_0, t) - E_g(n_0, t) = 0$] and one for hole excitations [where $E_h(n_0, t) - E_g(n_0, t) = 0$]. For each value of t there is a critical value of the chemical potential where the system changes phase from an incompressible to compressible fluid. The upper and lower curves for the Mott phase lobe are then described by this critical value of the chemical potential $\mu_{p/h}(t)$. The results of our expansion through third-order are

$$\begin{aligned}
\mu_p(t) &= n_0 + \epsilon(n_0 + 1)t - n_0(n_0 + 1)\epsilon^2 t^2 + \frac{n_0}{2}(5n_0 + 4)zt^2 \\
&\quad - n_0(n_0 + 1)[(2n_0 + 1)(-2 - \epsilon^2) + z(\frac{25}{4}n_0 + \frac{7}{2})]\epsilon t^3 \\
&\quad + 12\delta_{lat}n_0(\frac{31}{4}n_0^2 + \frac{21}{2}n_0 + 3)\cos(2\pi\phi)t^3 + O(t^4) \\
\mu_h(t) &= n_0 - 1 - \epsilon n_0 t + n_0(n_0 + 1)\epsilon^2 t^2 - \frac{n_0 + 1}{2}(5n_0 + 1)zt^2 \\
&\quad + n_0(n_0 + 1)[(2n_0 + 1)(-2 - \epsilon^2) + z(\frac{25}{4}n_0 + \frac{11}{4})]\epsilon t^3 \\
&\quad - 12\delta_{lat}(n_0 + 1)(\frac{31}{4}n_0^2 + 5n_0 + \frac{1}{4})\cos(2\pi\phi)t^3 + O(t^4), \tag{3}
\end{aligned}$$

where $\delta_{lat} = 0$ or 1 for the square or the triangular lattice, respectively, and z is the corresponding number of nearest neighbors (4 or 6, respectively). These results have been verified by both analytical small-cluster calculations and by numerical cluster expansions.

The magnetic field appears in two places: (1) The magnetic field couples to the orbital current of the bosons as the particle or hole travels around a lattice plaquette and encloses the flux $2\pi\phi$. In our third-order calculation, the orbital coupling only enters for the triangular lattice (it enters at fourth order for the square lattice as four hops are required to enclose a plaquette). (2) The other effect of the magnetic field is to change the minimal energy of the

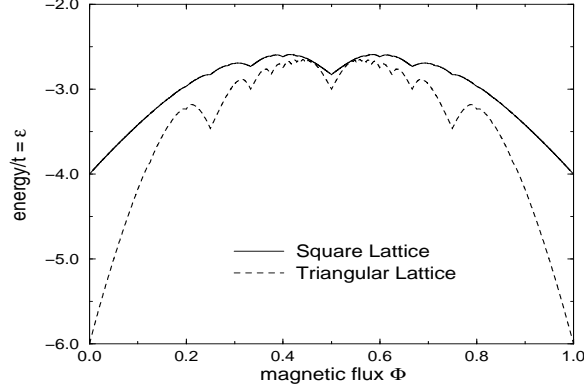


FIG. 1. Band minimum of the magnetic band structure $\epsilon(\phi)$ for the square and triangular lattice.

extra particle or hole moving in the Mott phase background. Although the location of this minimum in the Brillouin zone is gauge-dependent, its value is not (thus $\epsilon = \min_{\vec{k} \in \mathbb{B}} \epsilon(\vec{k})$).

We consider a rational flux $2\pi\phi = 2\pi p/q$. To find the minimal eigenvalues ϵt of the hopping matrix \hat{T} , we follow Bellisard⁹ and Hasegawa¹⁰. In the Landau gauge, the system maintains its translational invariance in the x -direction while it requires m steps for translational invariance in the y -direction. For the square lattice, the period m equals q , for the triangular lattice, $m = q/2$ for even q and $m = q$ for odd q . A Fourier-transformation now changes \hat{T} to the following $m \times m$ -matrix $\tilde{T}_\phi(\vec{k})$:

$$\tilde{T}_\phi(\vec{k}) = t \begin{pmatrix} M_1 & A_1 & 0 & & A_m^* \\ A_1^* & M_2 & \ddots & \ddots & \\ 0 & \ddots & \ddots & \ddots & 0 \\ & \ddots & \ddots & M_{m-1} & A_{m-1} \\ A_m & & 0 & A_{m-1}^* & M_m \end{pmatrix}, \quad (4)$$

with

$$M_n^{sq} = -2 \cos(k_y a + 2\pi n \phi), \quad A_n^{sq} = -e^{ik_x a}, \quad (5)$$

$$M_n^{tri} = -2 \cos(k_y a + 4\pi n \phi), \quad A_n^{tri} = -e^{ik_x a} (1 + e^{i2\pi\phi(2n+1) + ik_y a}). \quad (6)$$

The eigenvalues within the corresponding Brillouin-zone $\mathbb{B} = \{\vec{k} \mid 0 \leq k_x \leq 2\pi/m, 0 \leq k_y \leq 2\pi/m\}$ determine the m energy bands of a boson moving in the magnetic field. The minimal eigenvalue of the band-structure ϵt is shown in Fig. 1 as a function of the magnetic flux per plaquette $2\pi\phi$. This is the parameter that enters Eq. (3) to determine the Mott phase boundary. Notice how on the square lattice the largest dip is at $\phi = 1/2$ followed by $1/3$, $1/4$, and $2/5$, ... while on the triangular lattice the sequence corresponds to $1/2$, $1/4$, $1/3$, and $3/8$, ... The relation $\epsilon(\phi) = \epsilon(1 - \phi)$ holds for all lattices, since the flux of 2π is equivalent to a flux of 0. Hence, the maximal magnetic field that can be applied corresponds to $\phi = 1/2$. This maximal field configuration is realized by all real hopping matrix elements for each lattice: on the square lattice one takes three positive and one negative matrix element on each plaquette, while on the triangular lattice one takes all matrix elements to be negative. In particular, the “fully frustrated” case of $\phi = 1/2$ on a triangular lattice is the only nonzero magnetic-field case that can be easily treated by a high-order expansion¹² because it maintains the full periodicity of the triangular lattice in zero magnetic field.

Rather than plotting the phase diagrams for just a third-order expansion, we choose to extrapolate our results using knowledge about the overall structure of the phase diagram. There are numerous ways in which one can envision extrapolating the results of our third-order expansion to higher order. It has been demonstrated by Elstner and Monien that a Pade analysis of the strong coupling perturbation series yields rapid convergence in zero field¹². We apply this method to the magnetic-field case for small magnetic fields by using a Pade approximant¹³ for the logarithmic derivative of the difference in particle and hole Mott phase boundaries $\Delta(t) = \mu_p(t) - \mu_h(t)$. We assume

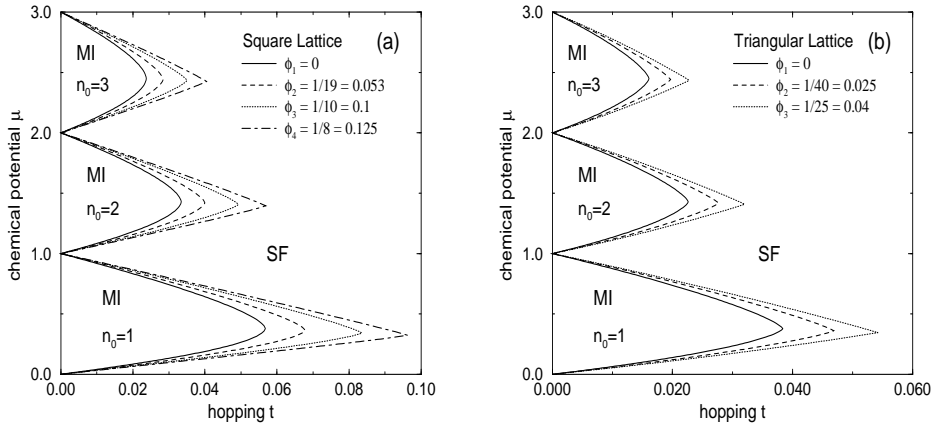


FIG. 2. Phase diagram for the square (a) and the triangular (b) lattice in relatively small magnetic fields using the Pade analysis.

the same behavior as found in the zero-field case, where the tip of the Mott lobe has a power law “critical point” with an exponent $z\nu$, $\Delta(t) = A(t)(t_{crit} - t)^{z\nu}$. Then the Pade analysis fits

$$\frac{\partial}{\partial t} \log \Delta(t) = \frac{z\nu}{t - t_{crit}} + \frac{A'(t)}{A(t)}, \quad (7)$$

to estimate the critical point and the dynamical critical exponent (the pole determines t_{crit} and the residue determines $z\nu$). The rest of the Pade approximant determines $A(t)$, which then allows $\Delta(t)$ to be constructed. A similar Pade analysis for the midline of the Mott lobe $\mu_m(t) = \frac{1}{2}[\mu_p(t) + \mu_h(t)]$ (which is a regular function of t) then allows the entire phase diagram to be constructed.

III. RESULTS

Atomic systems with a lattice spacing a of around 2\AA require a field of $H \cong 5 \times 10^3$ Tesla for a half flux quantum per plaquette. This is too large a field to be accessed experimentally, hence atomic systems always lie in the low-field region, where the perturbation theory is most accurate. However for macroscopic lattice systems, with $a \cong 2 \times 10^{-4} \text{cm}$ (as in a Josephson-junction array) the whole magnetic field range is attainable by experiments with fields as low as $H \cong 0.5$ Gauss. We show below how our theoretical results compare to the superfluid-insulator transitions on two dimensional Josephson-junction arrays⁵.

Fig. 2 presents the phase diagram of the first three lobes for the square lattice 2(a) and the triangular lattice 2(b) in the low magnetic-field region. The incompressible, Mott-insulating phase grows in size when the magnetic field increases from zero. This shows, as expected, the localizing effect of the magnetic field on the itinerant bosons. It appears that the shape of the lobes changes from a simple power-law dependence at the tip to something else. There are three possibilities for the shape of the phase lobe at the tip: (i) it remains power-law-like with an exponent that may depend on the magnetic field; (ii) it has a more exotic “cusp-like” dependence as seen in the Kosterlitz-Thouless transition; or (iii) it has a discontinuous change in slope at the tip, and thereby has a “first-order-like” shape corresponding to the crossing of the two curves representing the upper and lower phase lobes, with no “critical” behavior at the tip (this last result corresponds to $z\nu = 1$). There is theoretical evidence in favor of this last conclusion, which is a similar behavior to what happens to the MI phase in the presence of disorder, but here the explanation is different¹⁴. If $\phi = p/q$ is expressed in lowest terms, then the order parameter requires q components to describe it. As q increases, it is more likely that the transition is first-order rather than second-order, and hence one would expect that the tip has a slope discontinuity immediately upon the introduction of the magnetic field, since small fields correspond to large values of q . The Pade analysis given above assumes that (i) holds, but as $z\nu$ approaches 1 for larger fields, the system crosses over to the behavior of (iii) unless something more exotic like (ii) intervenes. We cannot distinguish between scenarios (i) or (iii) with the low-order expansions presented here, but our results suggest scenario (iii) is correct, because the exponent $z\nu$ rapidly approaches 1 as the field is increased. Clearly further theoretical analysis is needed to decide this issue.

For larger magnetic fields, we find that the two boundaries of the Mott phase lobe no longer cross at a critical value of t , but rather they “repeel” each other. This indicates that the tip of the MI phase lobe has moved out to such a large

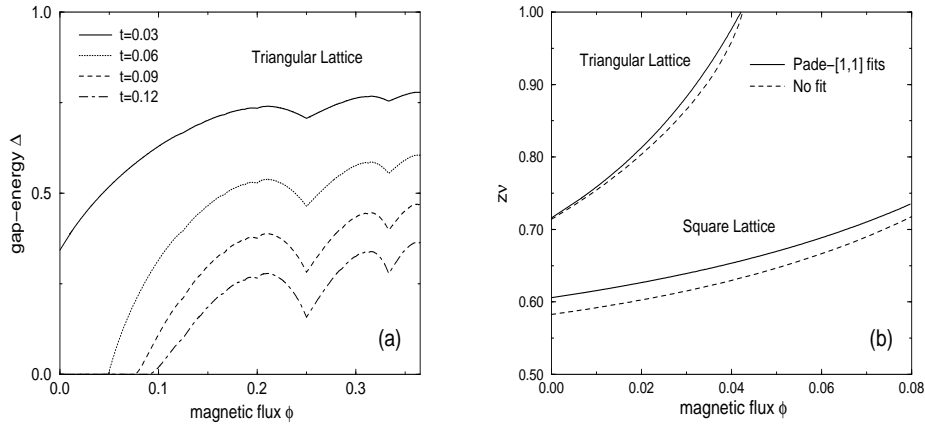


FIG. 3. (a) Dependence of the gap energy (for fixed hopping) on the magnetic field. Notice the kinks that develop at commensurate magnetic fields ($\phi = 1/3$ or $1/4$). The curves are cut off at $\phi \approx 0.35$ because the perturbation theory fails for larger values of ϕ . (b) Dependence of the dynamical critical exponent $z\nu$ on magnetic field when the truncated expansions, or a Pade approximant, are fit to the power-law behavior at the tip of the lobe. Notice that $z\nu$ appears to be field-dependent and rapidly approaches 1.

value of t that the perturbation theory needs to be carried out to higher order to achieve proper convergence. Such an exercise has been already carried out through a linked-cluster expansion for the fully frustrated case ($\phi = 1/2$) on a triangular lattice¹². The calculation from 3rd to 11th order converges toward a “first-order” transition ($z\nu = 1$) at $t_{crit} \approx 0.06$ which yields a much larger insulating phase regime than with no magnetic field where $t_{crit} \approx 0.038$. A comparable experimental result is found⁵ where the insulator to superfluid transitions on Josephson-junction arrays were studied by changing the ratio of the Josephson coupling energy E_J and the charging energy E_C . Since E_J is the energy scale for the superconducting coupling between the islands and E_C is the scale for the interaction between the charge carriers, they can be related to the hopping energy t and the on-site repulsion U , respectively. The results for small temperatures can be extrapolated to $T = 0$ and show a transition at larger E_J/E_C for the $\phi = 1/2$ case than for the $\phi = 0$ case, which qualitatively matches with our calculations (since t_{crit}/U increases with magnetic field).

The experimental data can be analyzed in one of two dual pictures with the Bose Hubbard model. In the first view, the bosons are the Cooper pairs on each island, and the main effect of the magnetic field is to modify the hopping matrix. Vortices appear in this case as supercurrent loops in the system. While the density of vortices increases as the magnetic field is modified, the density of Cooper pairs remains essentially constant over the low field ranges (on the order of Gauss) explored in the experiments. The second picture employs the duality transformation that views the vortices themselves as the bosonic particles¹⁶. The mobility of the vortices is determined by E_C and their interaction by E_J , so the roles of those parameters are reversed in this case. The magnetic field then takes on the role of the chemical potential. We will not employ this second picture here, which has been used to evaluate the Mott insulating phase of the vortices in the quasi-one-dimensional Josephson junction arrays¹⁷.

In the following we compare small-field results. As shown in Fig. 2 the MI phase area and the location of the tip of the lobe increase with increasing magnetic field up to about $\phi = 0.1$ (for the square lattice). The measurements of⁵ show $(E_J/E_C)_{crit} \approx 0.59$ and 0.83 for $\phi = 0$ and 0.1 respectively, which is similar to our results with t_{crit} increasing by about 45% from 0.057 to 0.083 as ϕ increases from 0 to 0.1 . In addition, the tip location for larger field strengths saturates in the experiments, which is a result that we cannot confirm, because our analysis through third-order in t fails when t_{crit} becomes too large.

In Fig. 3(a) we show the evolution of the excitation-gap energies $\Delta(t)$ for fixed hopping t as a function of magnetic field. Initially the gap energy increases which indicates the increasing stability of the MI phase in a weak magnetic field. For larger magnetic fields, we see dips in the gap energy around rational magnetic fluxes such as $\phi = 1/3$ or $1/4$ (which can be reliably calculated for small values of t). A similar commensurate structure is found in experiments that measure the zero-bias resistance (R_0) of a Josephson-junction array in a magnetic field⁵. A small R_0 indicates proximity to the SF phase. At rational ϕ the vortices form a lattice which is commensurate with the Josephson-junction array and favors a pinning of the vortices, leading to a decrease of the zero-bias resistance. Qualitatively, we see the same behavior in the excitation gap energies and the zero-bias resistance. Notice how the dips track closely with the dips seen in the minimal eigenvalue of the hopping matrix as shown in Fig. 1. This behavior explains the dips seen in the experimental data on the triangular lattice that are most prevalent at $1/2$, followed by $1/4$, $1/3$, $3/8$, and so on. The experimental data⁵ also shows that the system has four different regions of superconducting stability

for one value of t , centered at 0, 1/2, 1/4 and 1/3. While our results in Fig. 3(a) only show superconductivity around $\phi = 0$ [where $\Delta(t) = 0$], we can see that if t was increased, and the calculations carried out to higher order, it is likely that we would see additional superconducting regions appearing (we believe first around 1/2, followed by 1/4 and 1/3).

Finally we study the magnetic-field dependence of the dynamical critical exponent $z\nu$ (Eq. 7) for small fields in Fig. 3(b). The BHM in zero magnetic field can be mapped onto a three-dimensional XY model which has $z\nu = 0.67$ independent of the lattice structure¹⁹. By using the Pade analysis on our third-order expansion, we obtain $z\nu = 0.61$ for the square lattice and $z\nu = 0.72$ for the triangular lattice at $\phi = 0$. A Pade analysis of a tenth-order expansion¹² yields $z\nu = 0.69$ for both lattice types, which shows the convergence of higher-order calculations in our method. As seen in Fig. 3, the dynamical exponent appears to increase as the magnetic field increases. It is, however, difficult to conclude whether $z\nu$ remains equal to its zero-field value, increases with magnetic field, or immediately jumps to one upon the onset of a magnetic field, solely on the basis of this third-order analysis. But, the fact that the most likely point to have $z\nu < 1$ is $\phi = 1/2$ (because it requires only two components for the order parameter), and a higher-order expansion predicts $z\nu = 1$ there, leads us to conjecture that $z\nu = 1$ for all nonzero magnetic fields. This latter result is supported by Monte Carlo data on the antiferromagnetic XY model for stacked triangular planes, which have a weakly first-order transition rather than a critical point¹⁸.

IV. CONCLUSIONS

In conclusion, we applied a strong-coupling t/U -expansion (up to third order) to study the insulator-superfluid phase transitions of the two-dimensional Bose-Hubbard model under the influence of a magnetic field. Although our analysis is limited, we are able to produce reasonable results that both agree with physical intuition and with experiments. We found that the Mott insulating phase enlarges with an increasing magnetic field. This is explained by the localizing effect of the magnetic field on the moving bosons. Qualitative agreement in the increase of the critical hopping energy t_{crit} was found with experimental results on Josephson junction arrays⁵. For small magnetic fields, we find a power-law behavior of the gap energy close to the critical point (t_{crit}, μ_{crit}) with a dynamical critical exponent that increases with ϕ . For larger magnetic fields, we find a repulsion of the two phase boundaries, which indicates a change from the power-law like behavior to either Kosterlitz-Thouless behavior or to a “first-order” transition. Our results are also consistent with the “critical point” immediately changing to a “first-order” discontinuous change in the slope of the phase boundaries as the magnetic field is turned on. We found that the gap energies for small fixed hopping and variable magnetic field illustrate commensurability effects for rational fluxes which is also seen in Josephson-junction array experiments. More work is needed to understand the change in character of the insulator to superfluid phase transition as a magnetic field is introduced: does the system have a field-dependent power-law dependence which crosses over to a “first-order” (or more exotic cusp-like shape) as the field increases, or does it immediately become “first-order” in a field. Higher-order calculations are needed to decide this issue. It would also be interesting to extend the scaling analysis of the BHM to include its behavior in an external magnetic field.

ACKNOWLEDGMENTS

We would like to thank M. Ma for useful and interesting discussions. J.K.F. acknowledges support from an ONR YIP grant N000149610828 and from the Petroleum Research Fund administered by the American Chemical Society (ACS-PRF 29623-GB6).

¹ G. T. Zimanyi, P. A. Crowell, R. T. Scalettar and G. G. Batrouni, Phys. Rev. B **50**, 6515 (1994).

² H. M. Jaeger, D. B. Haviland, B. G. Orr and A. M. Goldman, Phys. Rev. B **40**, 182 (1989); Y. Liu and K. A. McGreer, B. Nease, D. B. Haviland, G. Martinez, J. W. Halley, and A. M. Goldman, Phys. Rev. Lett. **67**, 2068 (1991).

³ E. Roddick and D. Stroud, Phys. Rev. B **48**, 16600 (1993); *ibid.* **51**, 8672 (1995).

⁴ M. P. A. Fisher, P. B. Weichman, G. Grinstein, and D. S. Fisher, Phys. Rev. B **40**, 546 (1989).

⁵ H. S. J. van der Zant, F. C. Fritschy, W. J. Elion, L. J. Geerligs, and J. E. Mooij, Phys. Rev. Lett. **69**, 2971 (1992); H. S. J. van der Zant, W. J. Elion, L. J. Geerligs and J. E. Mooij, Phys. Rev. B **54**, 10081 (1996).

- ⁶ B. Pannetier, J. Chaussy, R. Rammal and J. C. Villegier, Phys. Rev. Lett. **53**, 1845 (1984); A. F. Hebard and M. A. Paalanen, ibid. **65**, 927 (1990); A. Yazdani and A. Kapitulnik, ibid. **74**, 3037 (1995).
- ⁷ J. K. Freericks and H. Monien, Europhys. Lett. **26**, 545 (1994); J. K. Freericks and H. Monien, Phys. Rev. B **53**, 2691 (1996).
- ⁸ D. R. Hofstadter, Phys. Rev. B **14**, 2239 (1976).
- ⁹ J. Bellissard, Ch. Kreft and R. Seiler, J. Phys. A **24**, 2329 (1990).
- ¹⁰ Y. Hasegawa, P. Lederer, T. M. Rice, P. B. Wiegmann, Phys. Rev. Lett. **63**, 907 (1989).
- ¹¹ F. H. Claro and G. H. Wannier, Phys. Rev. B **19**, 6068 (1979).
- ¹² N. Elstner and H. Monien, cond-mat/9807033.
- ¹³ A. J. Guttman in *Phase Transitions and Critical Phenomena*, edited by C. Domb and J. L. Lebowitz, Vol. 13 (Academic Press, London, 1989).
- ¹⁴ M. Ma, private communication.
- ¹⁵ M. P. Gelfand, R. R. P. Singh and D. A. Huse, J. Stat. Phys. **59**, 1093 (1990); M. P. Gelfand, Sol. State Commun. **98**, 11 (1996).
- ¹⁶ B. J. van Wees, Phys. Rev. B **44**, 2264 (1991).
- ¹⁷ A. van Oudenaarden and J. E. Mooij, Phys. Rev. Lett. **76**, 4947 (1996); A. van Oudenaarden, S. J. K. Várdu, and J. E. Mooij, ibid. **77**, 4257 (1996); A. van Oudenaarden, B. van Leeuwen, M. P. M. Robbens, and J. E. Mooij, Phys. Rev. B **57**, 11684 (1998).
- ¹⁸ M. L. Plumer, A. Mailhot, and A. Caillé, Phys. Rev. B **48**, 3840 (1993); ibid. **49**, 15133 (1994).
- ¹⁹ J. C. Le Guillou, and J. Zinn-Justin, Phys. Rev. Lett. **39**, 95 (1977).